

## Spin-Orbit Coupling and Tunneling Current in a Parabolic Quantum Dot

Hong-Yi Chen, Vadim Apalkov<sup>Y</sup>, and Tapash Chakraborty

Department of Physics and Astronomy, University of Manitoba, Winnipeg, MB R2T 2N2, Canada

<sup>Y</sup>Department of Physics and Astronomy, Georgia State University, Atlanta, Georgia 30303, USA

We propose a novel approach to explore the properties of a quantum dot in the presence of the spin-orbit interaction and in a tilted magnetic field. The spin-orbit coupling within the quantum dot manifest itself as anti-crossing of the energy levels when the tilt angle is varied. The anti-crossing gap has a non-monotonic dependence on the magnitude of the magnetic field and exhibits a peak at some finite values of the magnetic field. From the dependence of the tunneling current through the quantum dot on the bias voltage and the tilt angle, the anti-crossing gap and most importantly the spin-orbit coupling strength can be uniquely determined.

PACS numbers: 71.70.Ej, 73.40.Gk, 72.25.Dc

In recent years, there has been a well concerted effort to achieve a coherent control on the electron spin transport in semiconductor nanostructures because of its attractive potential for future spin-based electronic devices [1, 2]. The spin-orbit (SO) interaction plays a crucial role in that pursuit as it provides a means for coupling of the electron spin to its orbital motion. The SO interaction may in turn be manipulated by applying a gate voltage. Studies of the SO coupling effects in parabolic quantum dots are equally intriguing [3, 4] because it is expected that such a system will provide the important step toward the quantum information processing [5]. In narrow-gap semiconductors such as the InAs-based systems, the dominant source of the SO interaction is the structural inversion asymmetry [6]. The resultant Bychkov-Rashba type of SO interaction [7] is the interaction of our choice in the present investigation. The most common method of determining the strength of the SO coupling is to study the beating pattern in Shubnikov-de Haas (SdH) oscillations [8]. However, that process does not always provide an unambiguous determination of the SO coupling strength.

In this letter, we propose a new theoretical approach for measurement of the strength of the SO interaction in quantum dots. This approach is based on an analysis of the behavior of the electronic quantum dot energy levels in a tilted magnetic field. The tilted magnetic field has the distinct advantage over parallel and perpendicular fields because it introduces the Zeeman splitting of the energy levels and modifies the orbital motion of the electron within the quantum dot as well. The relative strength of these two contributions in the electron dynamics can be varied by changing the tilt angle. Without the SO interaction the energy spectrum of the quantum dot has a strong dependence on the direction of the magnetic field exhibiting regions of level crossings at different tilt angles. The levels that cross have the opposite spin directions, and without the SO interaction there is no mixing between them. Introducing the SO interaction results in a coupling between the different spin states. In this case we should expect an anti-crossing

of the energy levels as a function of the tilt angle. The strength of the anti-crossing characterizes the strength of the SO coupling. The most accurate way to study experimentally the structure of the energy spectra around the anti-crossing region is to measure the tunneling current through the quantum dot system. Transport spectroscopy is a powerful tool to study a variety of phenomena related to the correlation and interaction effects in a quantum dot [9, 10]. The main idea of the tunneling spectroscopy at a finite bias voltage is that the tunneling current depends on the number of available (for tunneling) channels in the quantum dot. In the following, we study the tunneling transport through a quantum dot in a tilted magnetic field and show that the tunneling current has a unique dependence on the tilt angle and the bias voltage within the anti-crossing region.

The energy range of the anti-crossing region is usually smaller than the energy of the inter-electron interaction, which can be estimated to be about 7 meV [4]. In that case we can describe the tunneling process by a single-electron picture. The Hamiltonian of an electron in a parabolic quantum dot in a tilted magnetic field has the form

$$H = \frac{1}{2m} p^2 + \frac{e}{c} \mathbf{A} \cdot \mathbf{p} + \frac{1}{2} m \omega_0^2 r^2 + \frac{1}{2} g_B B_z \sigma_z + \frac{1}{2} g_B B_x \sigma_x$$

Here,  $\mathbf{A} = \frac{1}{2} B_z (y; x; 0)$  is the vector potential in the symmetric gauge,  $\omega_0$  is the spin-orbital coupling strength,  $g$  is the effective Lande  $g$  factor, and  $\mathbf{p}$  is the two-dimensional vector in the  $(x; y)$  plane. In the above equation we assumed that there is no dynamics in the  $z$  direction due to the size quantization and the electron occupies the corresponding lowest subband. The value of  $\omega_0$  obtained from various experiments lie in the range of 5 { 45 meV nm [8]. In a tilted magnetic field, the perpendicular component is  $B_z = B \cos \theta$  while the parallel component is  $B_x = B \sin \theta$ , where  $B$  is the magnitude of magnetic field and  $\theta$  is the angle between the magnetic field vector and the  $z$ -axis. In the above expression for

the vector potential  $A$ , we have taken into account only the perpendicular component of the magnetic field  $B_z$ . Since the size of the dot in the  $z$  direction is small, the only effect of the parallel magnetic field is through the Zeeman energy. The energy spectra and the wavefunctions corresponding to the above Hamiltonian (but for a zero tilt angle) have been obtained numerically [4]. All the calculations below have been performed for the case of InAs quantum dots. It should be pointed out that tilted-field experiments on the quantum dots have been reported earlier in the literature [11], but in the absence of the SO coupling.

In our approach, a quantum dot is attached through the tunneling barriers to the right and left leads. We study the tunneling current through the dot at a finite bias voltage between the leads. We describe the process of tunneling through a parabolic quantum dot as a sequential single-electron tunneling [12]. The quantum dot system is characterized by the probability  $P_0$  that there are no electrons in the dot and probabilities  $P_i; i=1; \dots; N$  that the electron occupy an energy level  $E_i$  in the dot. For the probability  $P_i$  we can write the rate equations in the form

$$\frac{\partial P_0}{\partial t} = -\sum_{i=1}^N W_i P_0 + \sum_{i=1}^N P_i V_i; \quad (1)$$

$$\frac{\partial P_i}{\partial t} = P_i V_i + W_i P_0; \quad (2)$$

$$P_0 + P_1 + P_2 + \dots + P_N = 1; \quad (3)$$

where the last equation is the normalization condition. Here the transition rates  $W_i$  and  $V_i$  are the rates of tunneling in and out of the dot, respectively. These rates can be found from the Fermi golden rule

$$W_i = \Gamma_L(E_i) + \Gamma_R(E_i); \\ V_i = (\Gamma_L(E_i) + \Gamma_R(E_i));$$

where  $\Gamma$  is the tunneling rate, which we assume to be energy independent and is also the same for both left and right leads. Here  $\Gamma_L(E)$  and  $\Gamma_R(E)$  are the Fermi distribution functions of the left (L) and right (R) leads, respectively. The chemical potentials of the left and right leads are  $\mu_L$  and  $\mu_R$  respectively. In the calculations that follow, we have chosen the ground state of a quantum dot with a single electron as the zero-energy state. The temperature in our calculation is 10K.

For the stationary case, the time derivatives of  $P_0$  and  $P_i$  are zero. Then the linear system of equations Eqs. (1)-(3) can be easily solved and the stationary tunneling current can be found from the equation

$$I(V) = \sum_{i=1}^N W_i^L P_0 - V_i^L P_i;$$

where  $V$  is the bias voltage and the chemical potentials  $\mu_L$  and  $\mu_R$  are related to  $V$  as  $\mu_L = V/2$  and  $\mu_R = -V/2$ .

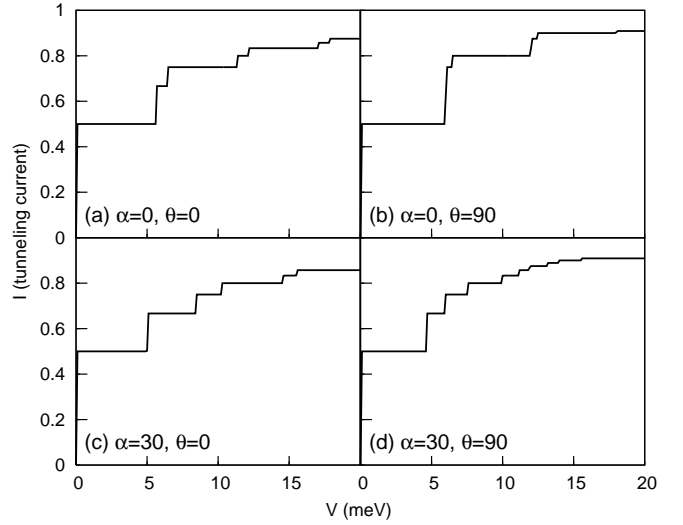


FIG. 1: Tunneling current vs the bias voltage for four different cases at  $B = 4$  Tesla: (a)  $\alpha = 0; \theta = 0$ ; (b)  $\alpha = 0, \theta = 90$ ; (c)  $\alpha = 30 \text{ m e V nm}^{-1}, \theta = 0$ ; (d)  $\alpha = 30 \text{ m e V nm}^{-1}, \theta = 90$ . The parameters for InAs quantum dots are  $m = m_0 = 0.042$ ,  $g = 14$ , and the confinement potential strength is  $\phi_0 = 3.0 \text{ m e V}$ .

In Fig. 1, we show the tunneling current as a function of the bias voltage for four different cases. The four cases can be divided into two groups by the angle of the applied tilted magnetic field: (i) ( $\theta = 0$ ) and (ii) ( $\theta = 90$ ). In the first case, Fig. 1 (a) and Fig. 1 (c) do not show any significant difference when the SO interaction is included, while in the second case the presence of the SO interaction lifts the degenerate states which creates more steps in the I-V curve [as seen in Fig. 1 (b) and Fig. 1 (d)].

From Fig. 1 it is clear that by varying the tilt angle one can make a significant change in the I-V curve. In order to study the effect of a tilted field, we have looked at the angle dependence of the energy levels. Figure 2 (a) shows several level crossing in the absence of the SO coupling. The first crossing appears around  $E = 4.5 \text{ m e V}$  and between  $70$  and  $90$ . In the presence of the SO coupling [Fig. 2 (b)], that level crossing becomes an anti-crossing with an energy gap of  $E$ . Figure 2 (c) shows that the energy gap increases with an increase of the strength of the SO coupling. The anti-crossing in Fig. 2 is a direct manifestation of the SO interaction. In what follows, we demonstrate that the anti-crossing of the energy levels results in a specific dependence of the tunneling current on the bias voltage and the tilt angle.

The tunneling current as a function of  $V$  is shown in Fig. 3. In Fig. 3 (a) we present the data for the tunneling current at different bias voltages with an increment of  $0.2 \text{ m e V}$  for the quantum dot without a SO coupling. At  $V = 8.6 \text{ m e V}$  ( $\mu_L = 4.3 \text{ m e V}$ ), the Fermi energy of the left lead  $\mu_L$  is below the first level crossing, which is illustrated by the dashed line in Fig. 2 (a). Around  $\theta = 70$ , there are three levels of the quantum dot below  $\mu_L$ . As we

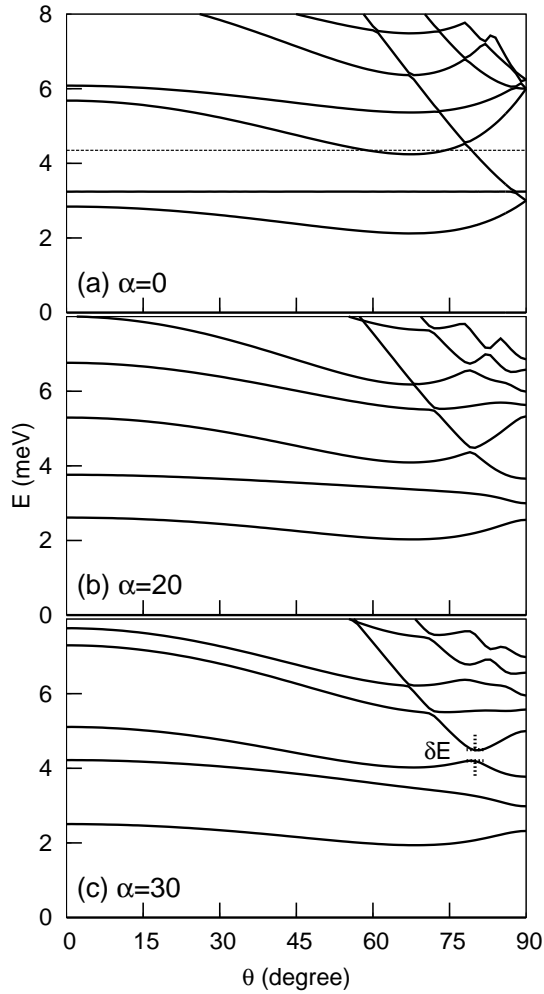


FIG. 2: The energy spectra as a function of the tilt angle ( $\theta$ ) for  $B = 4$  Tesla and for different values of the SO coupling strength: (a)  $\alpha = 0$ , (b)  $\alpha = 20$ , and (c)  $\alpha = 30$  m eV nm. The dashed line in (a) corresponds to the energy  $E = 4.3$  m eV. In (c),  $E_g$  is the energy gap.

increase the Fermi energy of the left lead goes below the third energy level. At this point, the tunneling current which depends on the number of levels between the Fermi energies of the left and right leads, drops. However, when  $\theta = 80^\circ$ , the Fermi energy  $E_L$  is again above the third energy level. The tunneling current then goes up. As a result, the tunneling current as a function of the tilt angle shows a dip at the voltage below the crossing point. When we increase the voltage and approach the crossing point, the dip becomes narrower. Just above the crossing point, the tunneling current shows a narrow bump similar to that at  $V = 9.2$  m eV in Fig 3(a). With a further increase of the bias voltage the bump in the tunneling current becomes wider.

Figure 3(b) shows the tunneling current for a finite value of the SO coupling strength  $\alpha = 30$  m eV nm. Just as for the system without the SO interaction, the tunneling current reveals a dip when the bias voltage is less

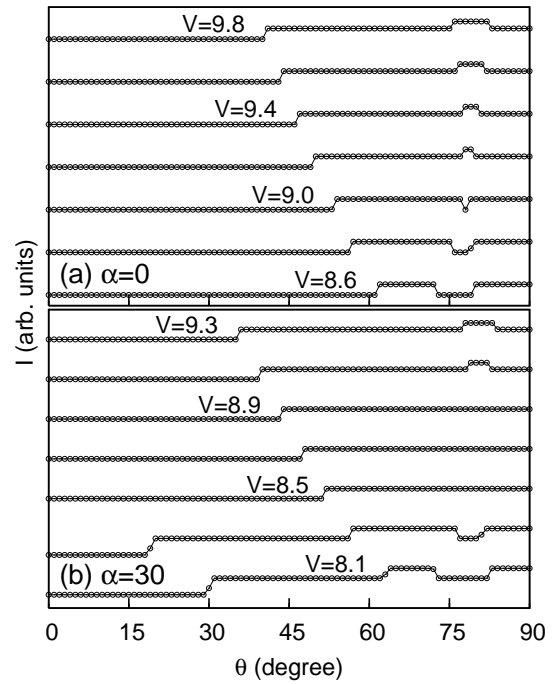


FIG. 3: Tunneling current as a function of the tilt angle at  $B = 4$  Tesla and for (a)  $\alpha = 0$ , and (b)  $\alpha = 30$  m eV nm. Each line corresponds to a constant bias voltage  $V$ . The bias voltage is expressed in m eV. The increment of the voltage is 0.2 m eV. The curves have been shifted vertically for clarity.

than 8.3 m eV. When the voltage is increased from that value, the system shows a behavior characteristic of that of the level anti-crossing. Namely, within a finite interval of the bias voltages  $V = 2 E_g$ , the tunneling current becomes independent of the tilt angle. This corresponds to the case where the Fermi energy of the left lead is in the anti-crossing gap. If the voltage is continuously increased, the dip pattern disappears and in its place a bump pattern emerges. Changing of the pattern reveals the evidence for the existence of the SO coupling which opens a gap at the crossing point [see Fig. 2(c)]. The dip occurs when the voltage is below the bottom edge of the energy gap, while the dip curve appears when the voltage is inside the gap. The bump in the curve means that the voltage is above the top edge of the energy gap. The change of pattern from a dip to being flat and then to a bump can be quantified by the voltage difference  $\Delta V$ . Since  $\Delta V = 2 E_g$ , this voltage difference will determine the strength of the SO coupling.

Analyzing the tunneling current as a function of the angles we are able to directly evaluate the strength of the SO coupling. However, the anti-crossing energy gap depends not only on the SO coupling strength but also on the magnitude of the applied magnetic field. With an increasing magnetic field the size of the energy gap increases and reaches a maximum value  $E_{max} = V_{max} = 2 E_g$ . Figure 4(a) illustrates the above trend for three different

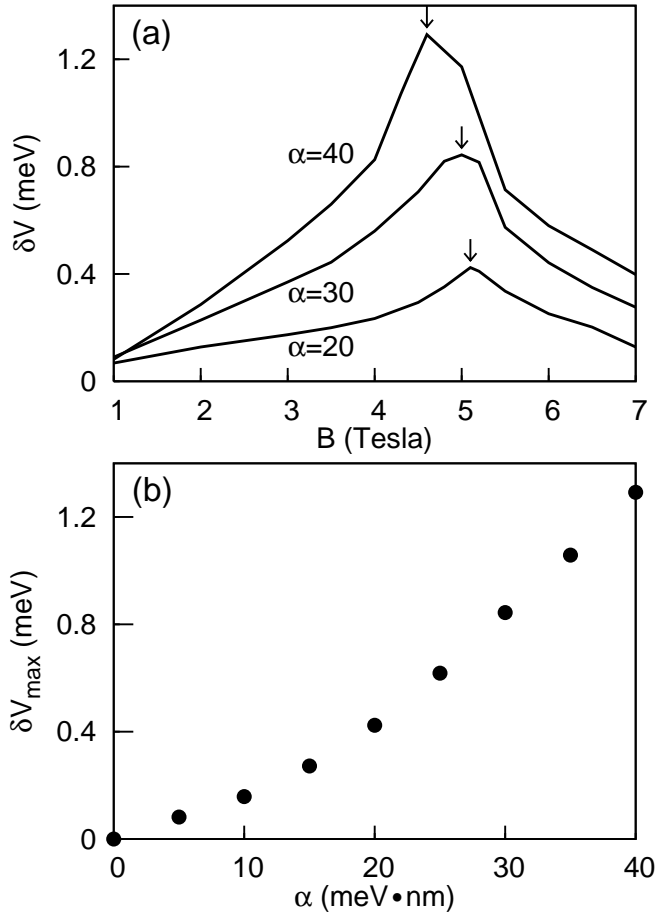


FIG. 4: (a) The magnetic field dependence of the voltage difference,  $V$  for three different values of the SO coupling strength:  $\alpha = 20, 30$ , and  $40$  meV nm. The corresponding peak positions are at  $B = 5.1, 5.0$ , and  $4.6$  Tesla for  $\alpha = 20, 30, 40$ , respectively. (b) The SO coupling strength dependence on the maximum voltage difference,  $V_{\max}$ . Each point corresponds to a different value of the magnetic field.

values of SO coupling strength. For larger values of the SO coupling strength, the peak is located at a lower magnetic field. The peak shifts toward a higher field as the SO coupling strength decreases. All the peak values are located between  $B = 4.5$  Tesla and  $B = 5.5$  Tesla. The optimal value of the magnetic field illustrates the interplay between the orbital and spin effects of the magnetic field. In Fig. 4 (b) the value of  $V_{\max}$  at the optimal magnetic field is shown as a function of the SO coupling. Note that at different values of the SO coupling the optimal magnetic field is different in Fig. 4 (b). With the known maximum value of the voltage differences,  $V_{\max}$ , the corresponding SO coupling strength can be directly determined.

In conclusion, the energy spectra of a quantum dot sys-

tem in a tilted magnetic field exhibits the anti-crossing behavior of the energy levels as a function of the tilt angle. The nature of anti-crossing of the energy levels is entirely due to the SO interaction. In the I-V characteristics of the tunneling current through the quantum dot the anti-crossing regions can be identified and the corresponding gap can be directly determined. The value of the gap has a strong dependence on the magnitude of the magnetic field and has a maximum at a finite value of the magnetic field. The anti-crossing gap exhibits a monotonic increase with an increase of the spin-orbit coupling strength.

HYC would like to thank P. Pietiläinen for helpful discussions. The work has been supported by the Canada Research Chair Program and a Canadian Foundation for Innovation Grant.

- 
- [1] D. D. Awschalom, D. Loss, and N. Samarth (Eds.), *Semiconductor Spintronics and Quantum Computation* (Springer, 2002); D. G. Rundler, *Phys. World* 15, 39 (2002); S. A. Wolf, D. D. Awschalom, R. A. Buhrman, J. M. Daughton, S. von Molnar, M. L. Roukes, A. Y. Chtchelkanova, and D. M. Treger, *Science* 294, 1488 (2001); G. A. Prinz, *Phys. Today* 48, 58 (1995).
- [2] *Proceedings of the First International Conference on the Physics and Applications of Spin Related Phenomena in Semiconductors*, edited by H. Ohno (*Physica E* 10 (2001)).
- [3] T. Chakraborty and P. Pietiläinen, *Phys. Rev. Lett.* 95, 136603 (2005); *Phys. Rev. B* 71, 113305 (2005).
- [4] P. Pietiläinen, T. Chakraborty, *Phys. Rev. B* 73, 155315 (2006).
- [5] M. A. Eriksson, et al., *Quantum Information Processing* 3, 133 (2004); D. Loss, G. Burkard, and D. P. DiVincenzo, *J. Nanoparticle Res.* 2, 401 (2000).
- [6] W. Zawadzki and P. Pfeffer, *Semicond. Sci. Technol.* 19, R1 (2004).
- [7] Yu. A. Bychkov and E. I. Rashba, *Pis'ma Zh. Eksp. Teor. Fiz.* 39, 64 (1984) [*JETP Lett.* 39, 78 (1984)].
- [8] D. G. Rundler, *Phys. Rev. Lett.* 84, 6074 (2000); J. Nitta, T. Akazaki, H. Takayanagi, and T. Enoki, *Phys. Rev. Lett.* 78, 1335 (1997); T. Matsuyama, C. M. Hu, D. G. Rundler, G. Meier, and U. Merkt, *Phys. Rev. B* 65, 155322 (2002).
- [9] J. Weis, R. J. Haug, K. von Klitzing, and K. Ploog, *Phys. Rev. Lett.* 71, 4019 (1993).
- [10] J. Koenig, R. J. Haug, D. K. Mauder, V. I. Fal'ko, and B. L. Altshuler, *Phys. Rev. Lett.* 94, 226404 (2005).
- [11] J. M. Mayer, I. Hapke-Wurst, U. Zeitler, R. J. Haug, and K. Ploog, *Phys. Stat. Sol. (b)* 224, 685 (2001); B. Meurer, D. Heitmann, and K. Ploog, *Surf. Sci.* 305, 610 (1994).
- [12] S. Luryi, *Appl. Phys. Lett.* 47, 490 (1985).